A Quick Test for Determination of N-Bombs (Phenethylamines Derivatives, NBOMe) Using High Performance Liquid Chromatography: A Comparison between Photodiode Array and Amperometric Detection

Hadil M. Elbardisy[1,2], Christopher W. Foster[1], Jack Marron,[1,3] Ryan E. Mewis,[1] Oliver B. Sutcliffe[1,3], Tarek S. Belal[4], Wael Talaat[2], Hoda G. Daabees[5] , Craig E. Banks[1*]

[1:] *Faculty of Science and Engineering, Manchester Metropolitan University, Chester Street, Manchester, M1 5GD, UK.*

[2:] *Pharmaceutical Analysis Department, Faculty of Pharmacy, Damanhour University, Damanhour, 22511, Egypt.*

[3:]*MANchesterDRug Analysis and Knowledge Exchange (MANDRAKE), Faculty of Science and Engineering, Manchester Metropolitan University, Chester Street, Manchester, M1 5GD, UK.*

[4:] *Department of Pharmaceutical Analytical Chemistry, Faculty of Pharmacy, Alexandria University, Alexandria, 21521, Egypt.*

[5:] *Pharmaceutical Chemistry Department, Faculty of Pharmacy, Damanhour University, Damanhour, 22511, Egypt.*

*To whom correspondence should be addressed.

Email: c.banks@mmu.ac.uk; Tel: ++(0)1612471196

Website: www.craigbanksresearch.com

Experimental

Instrumentation

Cyclic voltammetry (CV)

Voltammetric measurements were conducted using a 'μAutolab type III' (MetrohmAutolab, The Netherlands) potentiostat /galvanostat interfaced to a PC loaded with NOVA 2.1 software. All measurements were performed using a 10 mL voltammetric cell and a conventional three electrode system. A platinum wire was used as the counter electrode and Ag/AgCl was used as the reference electrode. Screen-printed graphite macroelectrodes (SPEs) with a 3.1 mm diameter working area were used as working electrodes [1, 2]. SPEs were fabricated in-house, as previously reported [3, 4], in Faculty of Science and Engineering, School of Science and the Environment, Division of Chemistry and Environmental Science, Manchester Metropolitan University.

Preparation of standard stock solutions and working solutions for cyclic voltammetry (CV)

10.0 mg of each NBOMe derivative (2a – 2d) were weighted separately into four 20.0 mL glass volumetric flasks and diluted to volume with ultrapure deionized water to obtain a stock solution of 0.5 mg mL^{-1} for each drug. Working solution of each drug was prepared by adding 1 mL of each drug stock solution to a 5.0 mL volumetric flask containing 4.0 mL of 0.04 M Britton-Robinson buffer (B-R, pH 7.0), to obtain a solution of 100 μg mL^{-1} of each drug. Each solution was transferred to a voltammetric cell, degassed with pure nitrogen for 10 minutes, and cyclic voltammograms were recorded between +0.5 to +1.2 V using scan rate 50 mV s^{-1}. A new SPE was used for each measurement and an overlay of cyclic voltammograms of the four derivatives was recorded.
The stock solutions were refrigerated at 4 °C for 2 weeks.

Preparation of selectivity standards

Adulterants commonly found in street samples(paracetamol, caffeine and benzocaine)

5.0 mg of each of paracetamol (**Pc**), caffeine (**Cf**), and benzocaine (**Bz**) were weighted separately into three 10.0 mL glass volumetric flasks and diluted to volume with the mobile phase to obtain a stock solution of 0.5 mg mL^{-1} for each compound. 1.0 mL from each stock solution was transferred separately into three 5.0 mL volumetric flasks, each flask was completed to volume with the mobile phase and injected into the HPLC to monitor the retention time (t_R) for each compound. Then, in order to test the possibility of interference of the selectivity standard compounds with the analysis of our analytes of interest, two test solutions were prepared. The first solution is prepared by addition of 1.0 mL of paracetamol (**Pc**) and 1.0 mL of benzocaine (**Bz**) to a 5.0 mL volumetric flask containing 1.0 mL of NBOMe standard stock solution (**S**), the flask was completed to the mark with the mobile phase and injected into the HPLC. The second solution was prepared in an analogous manner but paracetamol (**Pc**) was replaced with caffeine (**Cf**).

Preparation of specificity standards

5.0 mg of each of d-glucose, d-fructose, lactose, sucrose, starch, aerosil 200, stearic acid, sodium lauryl sulfate and sodium carboxymethyl cellulose were weighted accurately into one 10.0 mL glass volumetric flasks, dissolved in the mobile phase, sonicated for 20 minutes and diluted to volume with the same solvent

to obtain a stock solution of 0.5 mg mL^{-1} for each component. Three milliliters of the latter solution were transferred into a 5.0 mL volumetric flask, diluted to the mark with the mobile phase and injected into the HPLC. Another 3.0 mL of the excipient solution were added to a 5.0 mL volumetric flask containing 1 mL from the drug stock solution (**S**), the flask was mixed, made to the mark with the mobile phase and injected into the HPLC system.

Results and Discussion

Optimisation of the experimental and chromatographic conditions

Analytical column (Stationary phase)

In chromatographic analysis, the choice of column (packing material) is a key factor for the developed analytical methodology and it should make a compromise between the following chromatographic criteria: peak shape (sharp and symmetric), good separation and resolution (R_s) between peaks (ideally, R_s between successive peaks should be ≥ 2) and reasonable retention and run time. In our study, the tested stationary phases include: Greysil C8 (100 x 3.2 mm i.d., particle size: 5 µm), Eclipse XDB-C8 (150 x 4.6 mm i.d., particle size: 5 µm) and ACE 5 C18-AR (150 x 4.6 mm i.d., particle size: 5 µm). Regarding the total run time, all the tried columns retained the analytes of interest for long time and they demonstrated prolonged total analysis time (more than 15 minutes) when the mobile phase flow rate was less than 1.5 mL min^{-1}. This issue could be overcome by increasing the ratio of the organic modifier (acetonitrile) above 30%; however, this will be unfavorable for amperometric detection which prefers higher ratios of the aqueous phase for better electrical conductivity and improved amperometric sensitivity. Therefore, shorter analysis time was accomplished by increasing the flow rate beyond 1.5 mL min^{-1} together with increasing the column temperature, as described fully in the subsequent sections. Concerning the peak shape and symmetry, the first two columns eluted the analytes as tailed unsymmetrical peaks, in contrast with the third column, ACE 5 C18-AR (150 x 4.6 mm i.d., particle size: 5 µm), which gave sharp peaks with symmetry within the specified recommended values. Therefore, the third column was chosen for this study.

Mobile phase

By reviewing published papers for the chromatographic determination of NBOMe derivatives it was found that most of them have reported using ammonium acetate or ammonium formate as the aqueous phase and methanol or acetonitrile were used as the organic modifier. Hence, ammonium formate and acetonitrile were chosen as the components of the mobile phase. An isocratic system was favored over using a gradient program despite of its advantage in reducing the analysis time and optimising the separation and resolution between the eluted peaks. This was explained by Zuway *et al.* who adopted an isocratic methodology for HPLC-AD analysis of synthetic cathinones to provide a more stable constant baseline for amperometric detection and prevent the fluctuation of the electrolyte composition which can affect the electrochemical analysis sensitivity [3]. In addition, Zuway *et al.* isocratic mobile phase composed of reduced percentage of the organic modifier [10 mM ammonium acetate : methanol 70 : 30 % v/v] in combination with a suitable electrolyte (100 mM KCl) to enhance the electrochemical signal [3]. Likewise, in this study the mobile phase used was [5 mM ammonium formate + 100 mM KCl : acetonitrile 70 : 30 % v/v]. Attempts to decrease the percentage of the organic modifier were unfavorable as it prolonged the run time.

Ionic strength of ammonium formate buffer

The effect of the ionic strength of the used buffer was studied using 5, 10, 20 and 30 mM ammonium formate. In HPLC-DAD, it was found that increasing the molarity of the buffer, increases the baseline noise; the baseline noise increased significantly when using 30 mM of the formate buffer in addition to the possibility of its precipitation inside the column that may lead to its blockage. However, the peaks' shape and total run time were not affected by changing the buffer's molarity. In case of HPLC-AD, 5 mM ammonium formate provided the most sensitive amperometric signal for all the analytes, thereafter, the

measured current dropped when using 10 mM and did not change significantly at 20 and 30 mM of ammonium formate (**Figure S1A**). Thereby, 5 mM ammonium formate was the best buffer molarity for both detection systems.

pH of the aqueous phase

After selection of the best buffer and optimising its molarity, the effect of pH of the aqueous phase (5 mM ammonium formate + 100 mM KCl) was studied over the range 3 – 9 (at 1 pH unit increment). In HPLC-DAD, it was found that using pH 3 resulted in a very noisy baseline, however this noise decrease by increasing the pH from 4 till 9. Regarding the peak areas of the analytes, they remained nearly unchanged at all the studied pHs. The retention time and the total run time increased but not significantly from pH 3 till 8, however, pH 9 demonstrated longer retention times and prolonged run time (last peak eluted at 22.88 minutes). In case of HPLC-AD, pH 3.0 resulted in a very noisy baseline in the amperogram and no peaks for our analytes were detected (**Figure S1B**). By increasing the pH from 4 till 7, the amperometric current increased and reached a maximum value at pH 7 then the current dropped at pH 8 and 9 (**Figure S1B**). Thus, pH 7 was chosen as it gives the best compromise in terms of both amperometric and DAD sensitivity in addition to short analysis time.

Linear velocity of the mobile phase

After choosing the best mobile phase for this study and optimising it, the effect of its flow rate on the HPLC-DAD and HPLC-AD was studied in the range of 2.1 – 2.9 mL min^{-1} (in 0.2 mL min^{-1} increment). The tested flow rates were high to shorten the analysis time and elute the 4 derivatives within 10 minutes. In HPLC-DAD, it was found that changing the flow rate in this range did not affect the peak shape or symmetry and even the resolution (R_s) between the closest two eluting peaks in the chromatogram (25C-NBOMe and 25B-NBOMe) remained at 3.82. Concerning the sensitivity, the measured peak areas for all the analytes in HPLC-DAD were kept unchanged by varying the flow rate. Likewise, in HPLC-AD the measured peak heights were more or less similar for 25B-NBOMe **(2c)** and 25I-NBOMe **(2d)** but changed considerably in case of 25F-NBOMe **(2a)** and 25C-NBOMe **(2b)** (**Figure S1C**), and flow rate of 2.5 mL min^{-1} demonstrated a better sensitivity. Therefore, flow rate 2.5 mL min^{-1} was chosen for this study.

Column Temperature

Different column temperatures were tried in order to improve the peaks' sharpness and shorten the total analysis time. The studied temperatures were: ambient temperature 25, 30, 40 50 and 60 °C. It was found that lower temperatures, 25 - 40 °C, affected the peak symmetry of the first peak (25F-NBOMe, **2a**) either by tailing or fronting and increasing the temperature enhanced its sharpness and symmetry a lot, whilst the other peaks were sharp and symmetric at all the tried temperatures. Another point worth mentioning is that the total run time was reduced from 18.0 till 10.0 minutes by increasing the column temperature from 25 till 60 °C, which is preferred and save the total analysis time. Regarding the sensitivity, the analytes' peak areas in HPLC-DAD were kept nearly the same in all temperatures, whilst in HPLC-AD, 25F- and 25C-NBOMe (**2a** and **2b**) were slightly more affected by changing the column temperature than the other derivatives (**Figure S1D).** Consequently, temperature 60 °C was chosen for better peak symmetry, shorter analysis time and better amperometric sensitivity.

Optimisation of the applied potential for high performance liquid chromatography-amperometric detection (HPLC-AD)

The applied potential has to be optimised in order to enhance the sensitivity of the amperometric detection. From the data we obtained from cyclic voltammetry (CV) (**Figure 1**), it was apparent that all the

NBOMe derivatives have two anodic peaks; the first at $E_p \approx +0.81$ V and the second at $E_p \approx +1.02$ V. Reliably, in order to maximize the assay sensitivity we used a potential where all the drugs are completely oxidized and the two oxidation steps have occurred. Thus the amperometric response (peak current, µA) was measured as a function of the applied potential (E V^{-1}) over the range (E_p= +0.8 to +1.2 V, in 0.1 V increment). A weak current was induced by all the analytes upon using a potential of +0.8 V, however, this current increased gradually and reached a maximum value at E_p= +1.0 V (**Figure S1E**). Afterwards, increasing the applied potential from + 1.0 V till +1.2 V resulted in increasing the baseline noise and decreasing amperometric response for 25F- and 25C-NBOMe (**2a** and **2b**), while a plateau was reached for 25B- and 25I-NBOMe (**2c** and **2d**) (**Figure S1E**). Consequently, a potential equivalent to +1.0 V was chosen and applied in our study.

Optimisation of the detection wavelength for high performance liquid chromatography-photodiode array detection (HPLC-DAD)

In order to quantify NBOMe halide derivatives accurately and maximize the HPLC-DAD assay sensitivity, the DAD detector should be set at the wavelength of maximum absorption for each compound (λ_{max}). Because the literature is scarce with respect to the UV absorption spectra and λ_{max} of NBOMe derivatives, the UV absorption spectrum of 10 µg mL^{-1} of each derivative was measured in the optimised mobile phase as shown in **Figure S2**. It is depicted in **Figure S2** that all the derivatives have a maximum peak (λ_{max}) at around 205 nm which was chosen for the HPLC-DAD measurement of NBOMe derivatives and provided higher peak areas in comparison to other tested wavelengths (λ = 210, 230, 254, and 280 nm).

Validation of the proposed method

Selectivity tests for adulterants commonly found in street samples (paracetamol, caffeine and benzocaine)

Beside testing the selectivity of the proposed protocol using LSD, selectivity was further assessed by injecting potential adulterants commonly found in street samples, which are paracetamol (**Pc**), caffeine (**Cf**) and benzocaine (**Bz**), these adulterants are both UV and electrochemically active. 100 µg mL^{-1} of each adulterant were injected alone and their retention times, in HPLC-DAD, were detected as follows: 0.77 ± 0.03 min for (**Pc**), 0.86 ± 0.05 min for (**Cf**) and 2.45 ± 0.06 min for (**Bz**). For HPLC-AD, the retention times were: 0.78 ± 0.05 min for (**Pc**), 0.87 ± 0.07 min for (**Cf**) and 2.46 ± 0.08 min for (**Bz**). Unfortunately, the chromatographic method could not make a sufficient separation or efficiently resolve paracetamol (**Pc**) and caffeine (**Cf**) peaks in the same chromatographic run (R_s factor between the 2 peaks = 1.12), as the two peaks elute at close retention times. Wherefore, two adulterated solutions were prepared; one containing 100 µg mL^{-1} of each of paracetamol (**Pc**), benzocaine (**Bz**) and the four NBOMe derivatives, while the second solution was the same but paracetamol (**Pc**) was substituted with caffeine (**Cf**). **Figures 3SA** and **3SB** present the HPLC-DAD chromatogram and HPLC-AD amperogram for the first adulterated solution, respectively, and **Figures 3SC** and **3SD** depict the HPLC-DAD chromatogram and HPLC-AD amperogram for the second adulterated solution. HPLC-DAD chromatograms (**Figures 3SA and 3SC**) demonstrate that the resolution (R_s) between paracetamol (**Pc**) and/or caffeine (**Cf**) and the next eluted peak, benzocaine (**Bz**) peak, correspond to 18.23 and 17.17 respectively. Whereas, in these chromatograms, the resolution between benzocaine (**Bz**) and the following peak, 25F-NBOMe **(2a)**, is equivalent to 9.1, which demonstrates the success of the method in separation of the NBOMe halide derivatives from common street sample adulterants. HPLC-DAD chromatogram, presented in **Figure 3SC**, shows a peak for caffeine (**Cf**) and a peak for benzocaine (**Bz**) while HPLC-AD amperogram, illustrated in **Figure 3SD**, gives rise to a sole peak for benzocaine (**Bz**). The disappearance of caffeine (**Cf**) peak is due to the fact that caffeine (**Cf**) undergoes

irreversible electrochemical oxidation at a potential $E_p \approx +1.4$ V and a favorable pH for this oxidation to occur is pH ≈ 4.5[5, 6], however, herein, HPLC-AD measurements were conducted at a potential $E_p = +1.0$ V (*vs*. Ag/AgCl) and a pH of 7.0. Thus, changing both factors (the applied potential and the buffer pH) precluded the oxidation of caffeine (**Cf**).

Specificity test employing pharmaceutical excipients and diluents

The specificity of the developed method was investigated by injecting a solution containing 300 µg mL^{-1} of potential excipients commonly found in pharmaceutical formulations (d-glucose, d-fructose, lactose, sucrose, starch, aerosil 200, stearic acid, sodium lauryl sulfate and sodium carboxymethyl cellulose). It was found that this solution did not show any peak either in HPLC-DAD chromatogram (**Figure S4A**) or in HPLC-AD amperogram (**Figure S4B**) over the entire run time. Moreover, a solution containing 300 µg mL^{-1} of excipients and 100 µg mL^{-1} of the analytes of interest was injected into the HPLC and the magnitude of the response (peak area and peak heights) of each drug was measured by both detectors and compared to their responses in absence these pharmaceutical excipients. It was found that the added excipients did not interfere and did not affect the analytical sensing of the investigated drugs by both detectors; the additives added were UV-inactive and electrochemically inert. This demonstrates the high specificity and selectivity of the developed sensing protocol.

Table S1. Evaluation of the robustness of the proposed HPLC-DAD system **(Detection System I)** for the determination of NBOMe halide derivatives **(2a – 2d)**.

Drug of abuse / Parameters	25F-NBOMe (2a)	25C-NBOMe (2b)	25B-NBOMe (2c)	25I-NBOMe (2d)
Mean % recovery ± SD[a]				
Temperature (60 °C ± 2°C)	98.57 ± 1.44	99.98 ± 0.21	100.15 ± 0.24	99.35 ± 0.09
Molarity of buffer (5 ± 2.0)	100.33 ± 0.85	100.37 ± 0.52	99.62 ± 0.53	99.74 ± 0.55
pH of buffer (7.0 ± 0.2 pH units)	100.22 ± 0.56	100.43 ± 0.33	100.80 ± 0.94	99.70 ± 1.78
RSD%[b]				
Temperature (60 °C ± 2°C)	1.46	0.21	0.24	0.09
Molarity of buffer (5 ± 2.0)	0.85	0.52	0.53	0.55
pH of buffer (7.0 ± 0.2 pH units)	0.56	0.33	0.93	1.79
t_R±SD[c]				
Temperature (60 °C ± 2°C)	3.83 ± 0.04	5.96 ± 0.04	7.01 ± 0.08	9.45 ± 0.10
Molarity of buffer (5 ± 2.0)	3.83 ± 0.13	5.96 ± 0.29	7.01 ± 0.44	9.45 ± 0.58
pH of buffer (7.0 ± 0.2 pH units)	3.83 ± 0.05	5.96 ± 0.08	7.01 ± 0.09	9.45 ± 0.11

[a] Mean ± SD of percentage recoveries of peak areas of each drug at the three studied parameters.

[b] Percentage relative standard deviation of peak areas of each drug at the three studied parameters.

[c] Mean ± SD of retention time of each drug at the three studied parameters.

Table S2. Evaluation of the robustness of the proposed HPLC-AD system **(Detection System II)** for the determination of NBOMe halide derivatives **(2a – 2d)**.

Drug of abuse / Parameters	25F-NBOMe (2a)	25C-NBOMe (2b)	25B-NBOMe (2c)	25I-NBOMe (2d)
Mean % recovery ± SD[a]				
Temperature (60 °C ± 2°C)	100.29 ± 0.57	100.28 ± 1.14	99.27 ± 0	100.19 ± 0.05
Molarity of buffer (5 ± 2.0)	100.02 ± 1.06	99.70 ± 1.32	101.00 ± 0.54	99.00 ± 1.74
pH of buffer (7.0 ± 0.2 pH units)	99.92 ± 0.96	99.70 ± 0.25	99.60 ± 0.79	100.39 ± 0.69
RSD%[b]				
Temperature (60 °C ± 2°C)	0.57	1.14	0	0.05
Molarity of buffer (5 ± 2.0)	1.06	1.32	0.53	1.76
pH of buffer (7.0 ± 0.2 pH units)	0.96	0.25	0.79	0.69

[a] Mean ± SD of percentage recoveries of peak areas of each drug at the three studied parameters.

[b] Percentage relative standard deviation of peak areas of each drug at the three studied parameters.

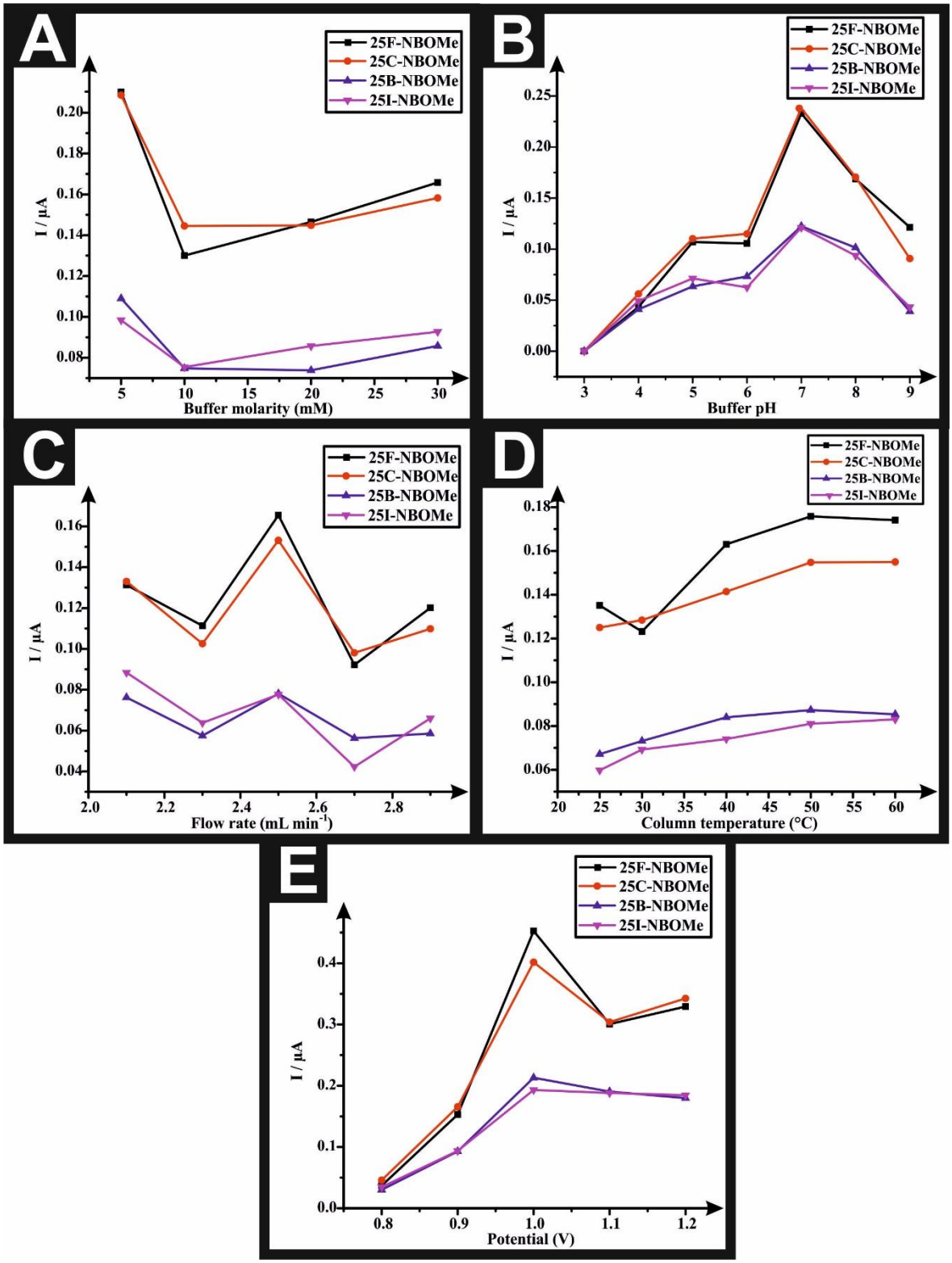

Figure S1. Effect of **(A)** buffer molarity (mM), **(B)** buffer pH, **(C)** mobile phase flow rate (mL min^{-1}), **(D)** column temperature (°C), **(E)** applied potential (E/V) on the measured current intensity in HPLC-AD system.

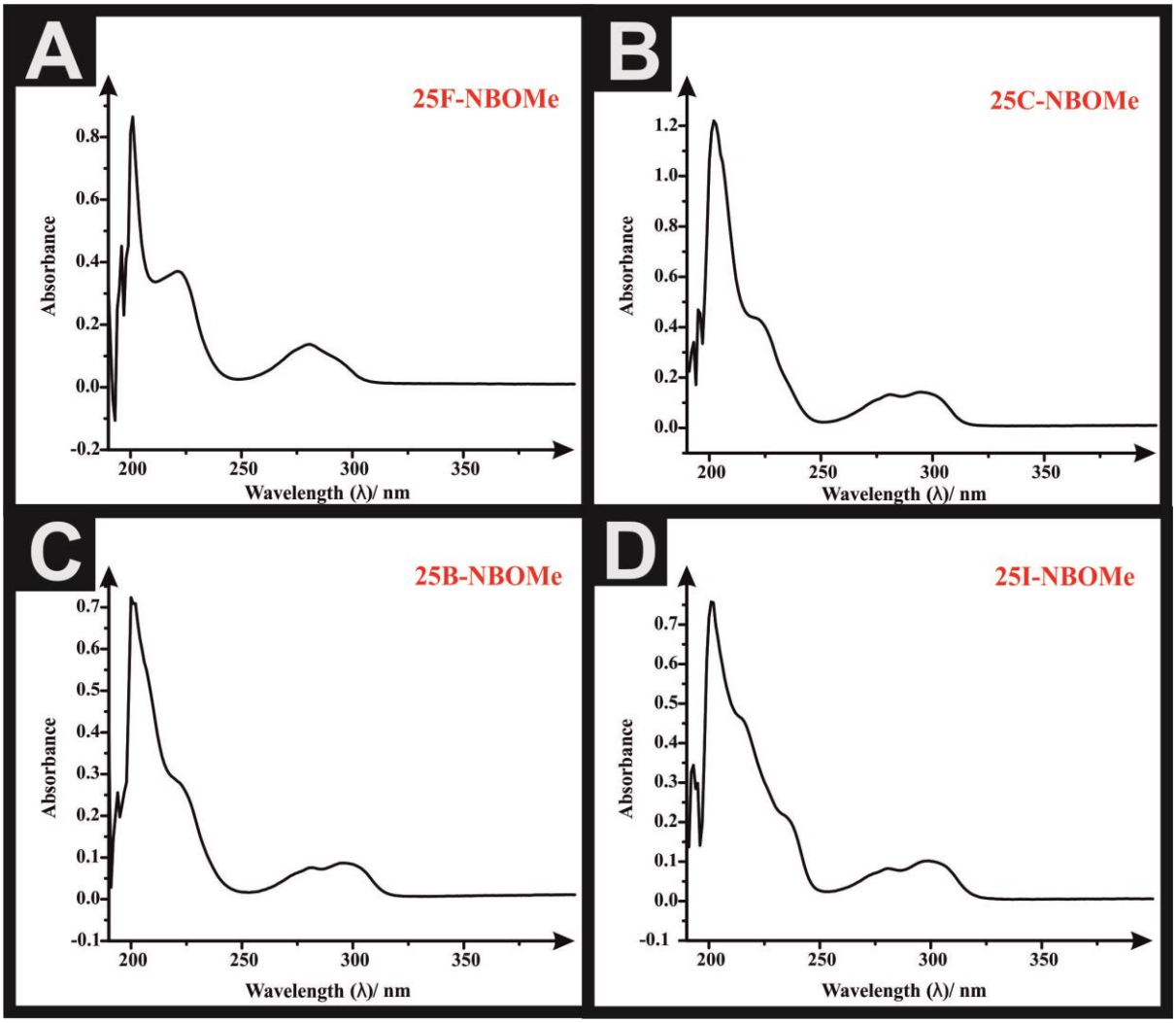

Figure S2. UV absorption spectra of 10 µg mL^{-1} of **(A)** 25F-NBOMe (**2a**), **(B)** 25C-NBOMe (**2b**), **(C)** 25B-NBOMe (**2c**) and **(D)** 25I-NBOMe (**2d**) in solutions of the mobile phase showing their λ_{max} at 205 nm.

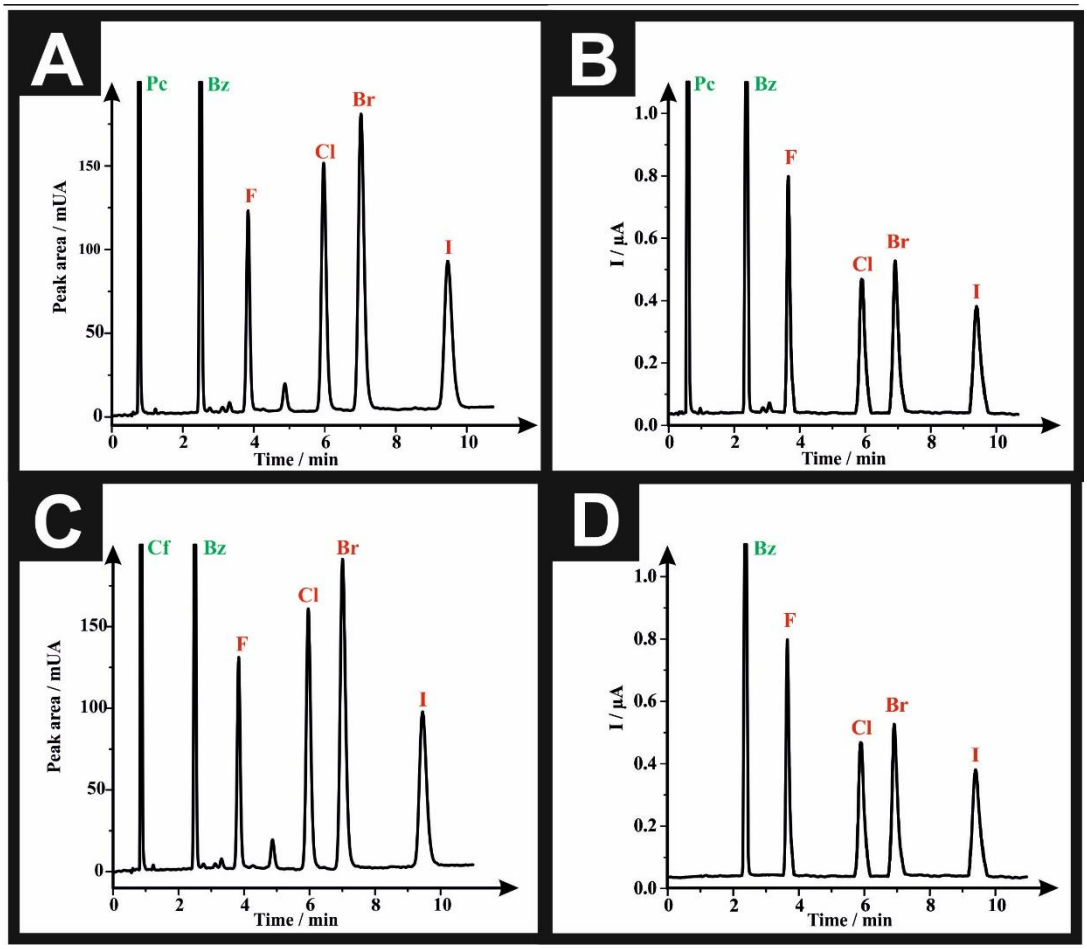

Figure S3. (A) Representative HPLC-DAD chromatogram and **(B)** representative HPLC-AD amperogram of a solution containing 100 µg mL^{-1} of each paracetamol (**Pc**), benzocaine (**Bz**), **"F":** 25F-NBOMe **(2a)**, **"Cl":** 25C-NBOMe **(2b)**, **"Br":** 25B-NBOMe **(2c** and **"I":** 25I-NBOMe**(2d)**. **(C)** Representative HPLC-DAD chromatogram and **(D)** representative HPLC-AD amperogram of a solution containing 100 µg $mL^{-1}$of each of caffeine (**Cf**), benzocaine (**Bz**), **"F":** 25F-NBOMe **(2a)**, **"Cl":** 25C-NBOMe**(2b)**, **"Br":** 25B-NBOMe **(2c)** and **"I":** 25I-NBOMe **(2d)**. Experimental conditions include: ACE C18-AR column (150 x 4.6 mm i.d., particle size: 5 µm), mobile phase: [5 mM ammonium formate + 100 mM KCl (pH 7.0): acetonitrile 70:30 % (v/v)], flow rate 2.5 mL/min, column temperature: 60 °C, detector wavelength (UV): 205 nm and potential = +1.0 V. Note that in figure **(D)** caffeine (Cf) peak did not appear.

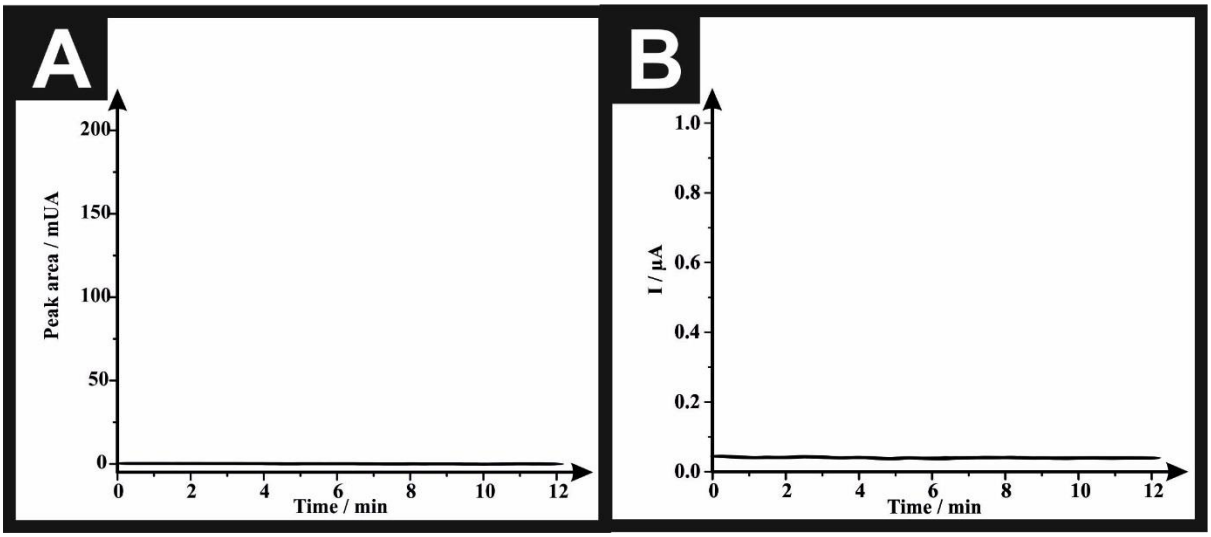

Figure S4. (A) Representative HPLC-DAD chromatogram **(B)** Representative amperogram for a solution containing 300 µg mL^{-1} of each of d-glucose, d-fructose, lactose, sucrose, starch, aerosil 200, stearic acid, sodium lauryl sulfate and sodium carboxymethyl cellulose using ACE C18-AR column (150 x 4.6 mm i.d., particle size: 5 µm), mobile phase: [5 mM ammonium formate + 100 mMKCl (pH 7.0): acetonitrile; 70:30 % (v/v)], flow rate 2.5 mL min^{-1}, column temperature: 60 °C, detector wavelength: 205 nm and potential = +1.0 V.

Figure S5. [1]H-NMR (400 MHz, d4-MeOH) spectra of 2-(4-fluoro-2,5-dimethoxyphenyl)-N-(2-methoxybenzyl)ethan-1-amine.HCl (**2a**, 25F-NBOMe.HCl) [TOP] and 2-(4-chloro-2,5-dimethoxyphenyl)-N-(2-methoxybenzyl)ethan-1-amine.HCl (**2b**, 25C-NBOMe.HCl) [BOTTOM].

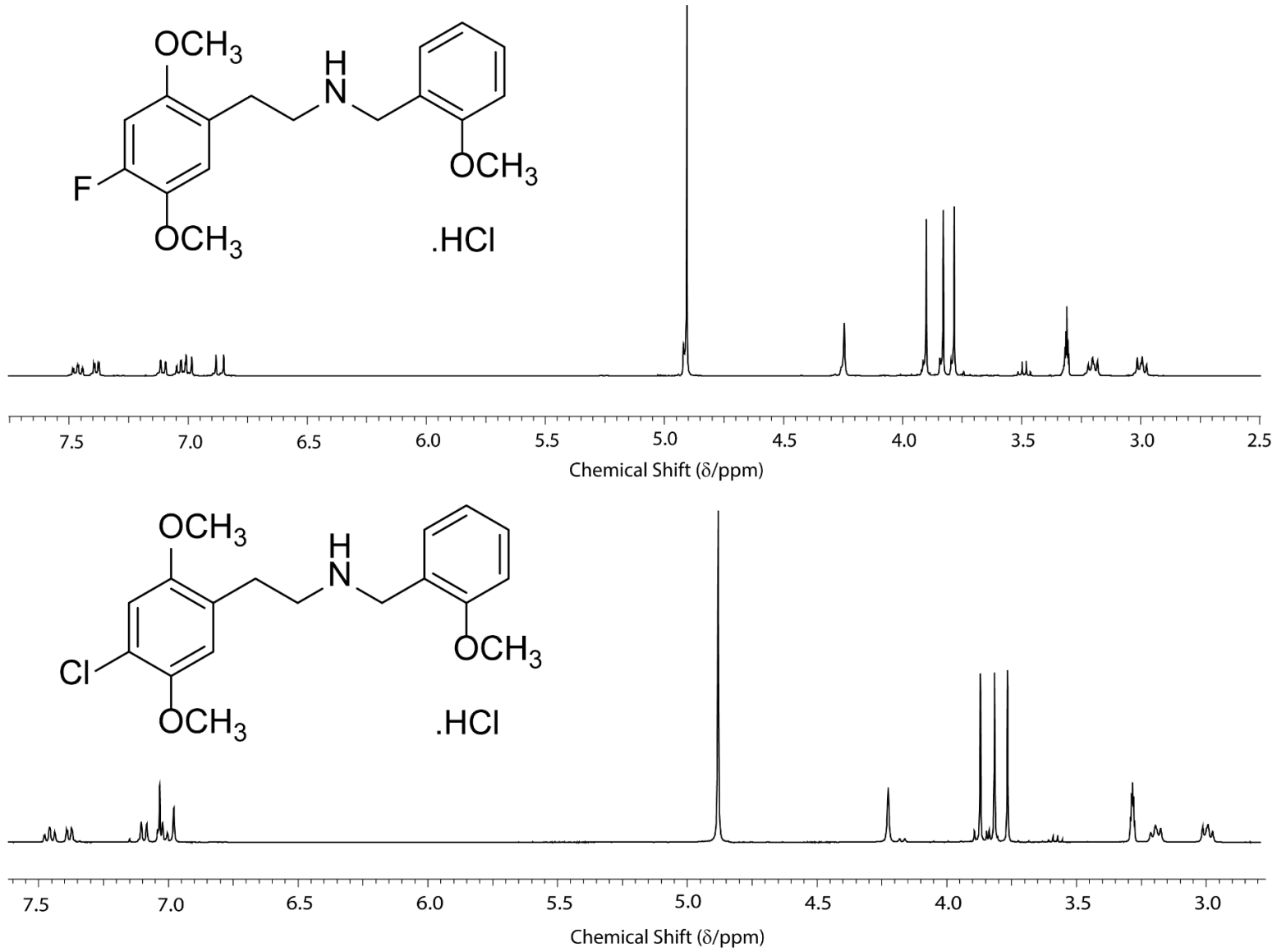

Figure S6. ^{1}H-NMR (400 MHz, d_4-MeOH) spectra of 2-(4-bromo-2,5-dimethoxyphenyl)-N-(2-methoxybenzyl)ethan-1-amine.HCl (**2c**, 25B-NBOMe.HCl) [TOP] and 2-(4-iodo-2,5-dimethoxyphenyl)-N-(2-methoxybenzyl)ethan-1-amine.HCl (**2d**, 25I-NBOMe.HCl) [BOTTOM].

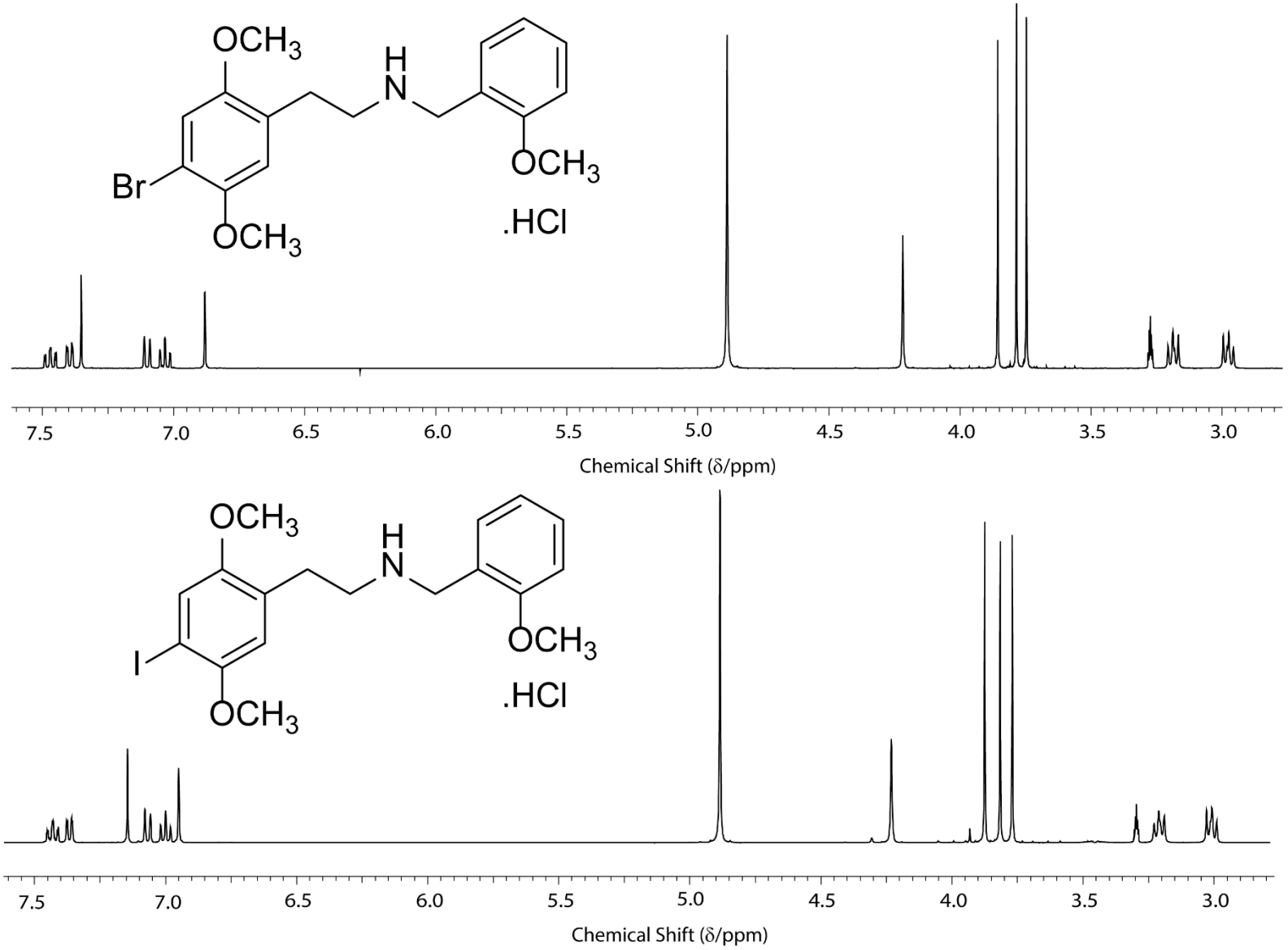

Figure S7. ^{13}C-NMR (100 MHz, d_4-MeOH) spectra of 2-(4-fluoro-2,5-dimethoxyphenyl)-N-(2-methoxybenzyl)ethan-1-amine.HCl (**2a**, 25F-NBOMe.HCl) [TOP] and 2-(4-chloro-2,5-dimethoxyphenyl)-N-(2-methoxybenzyl)ethan-1-amine.HCl (**2b**, 25C-NBOMe.HCl) [BOTTOM].

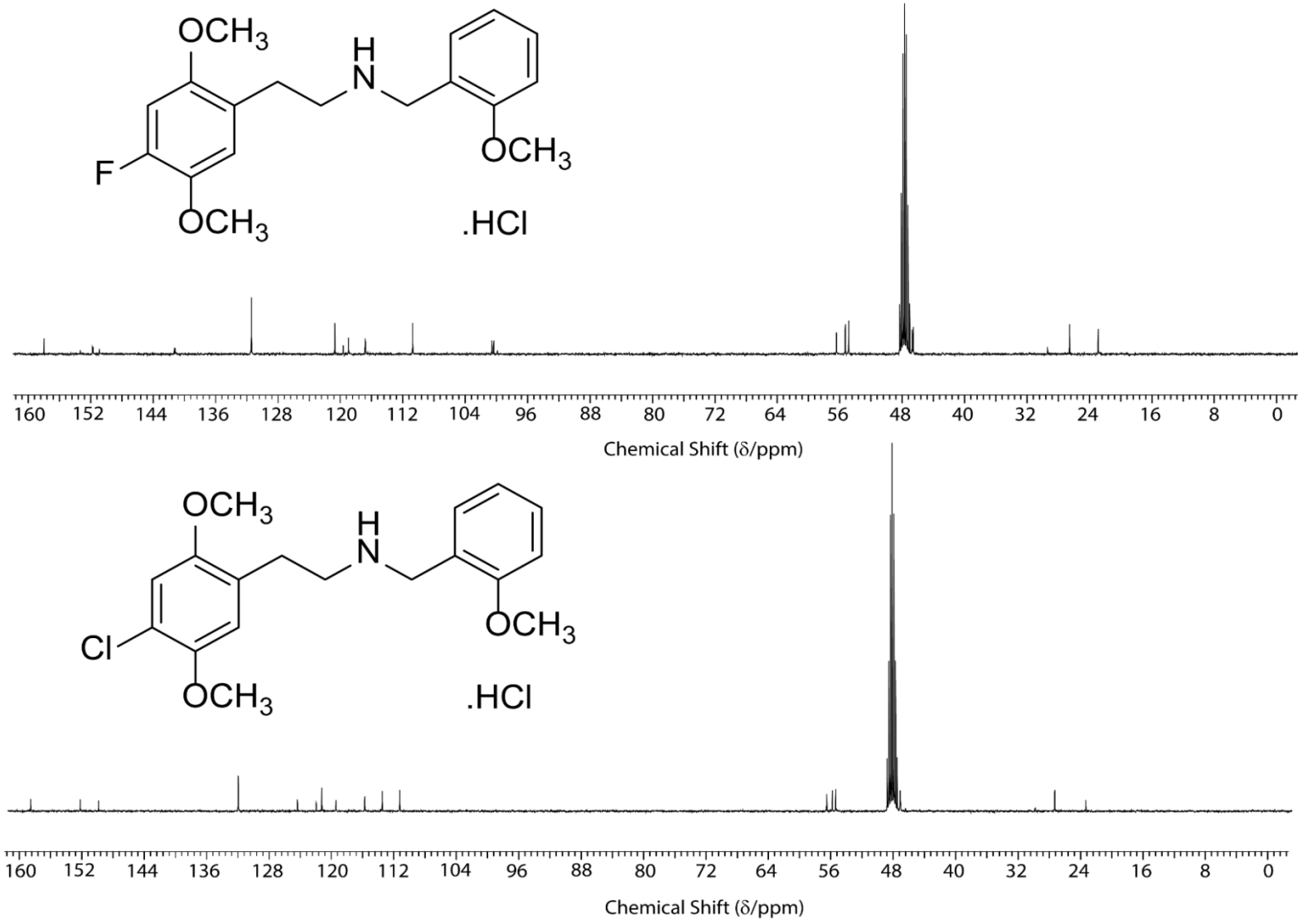

Figure S8. ^{13}C-NMR (100 MHz, d_4-MeOH) spectra of 2-(4-bromo-2,5-dimethoxyphenyl)-N-(2-methoxybenzyl)ethan-1-amine.HCl (**2c**, 25B-NBOMe.HCl) [TOP] and 2-(4-iodo-2,5-dimethoxyphenyl)-N-(2-methoxybenzyl)ethan-1-amine.HCl (**2d**, 25I-NBOMe.HCl) [BOTTOM].

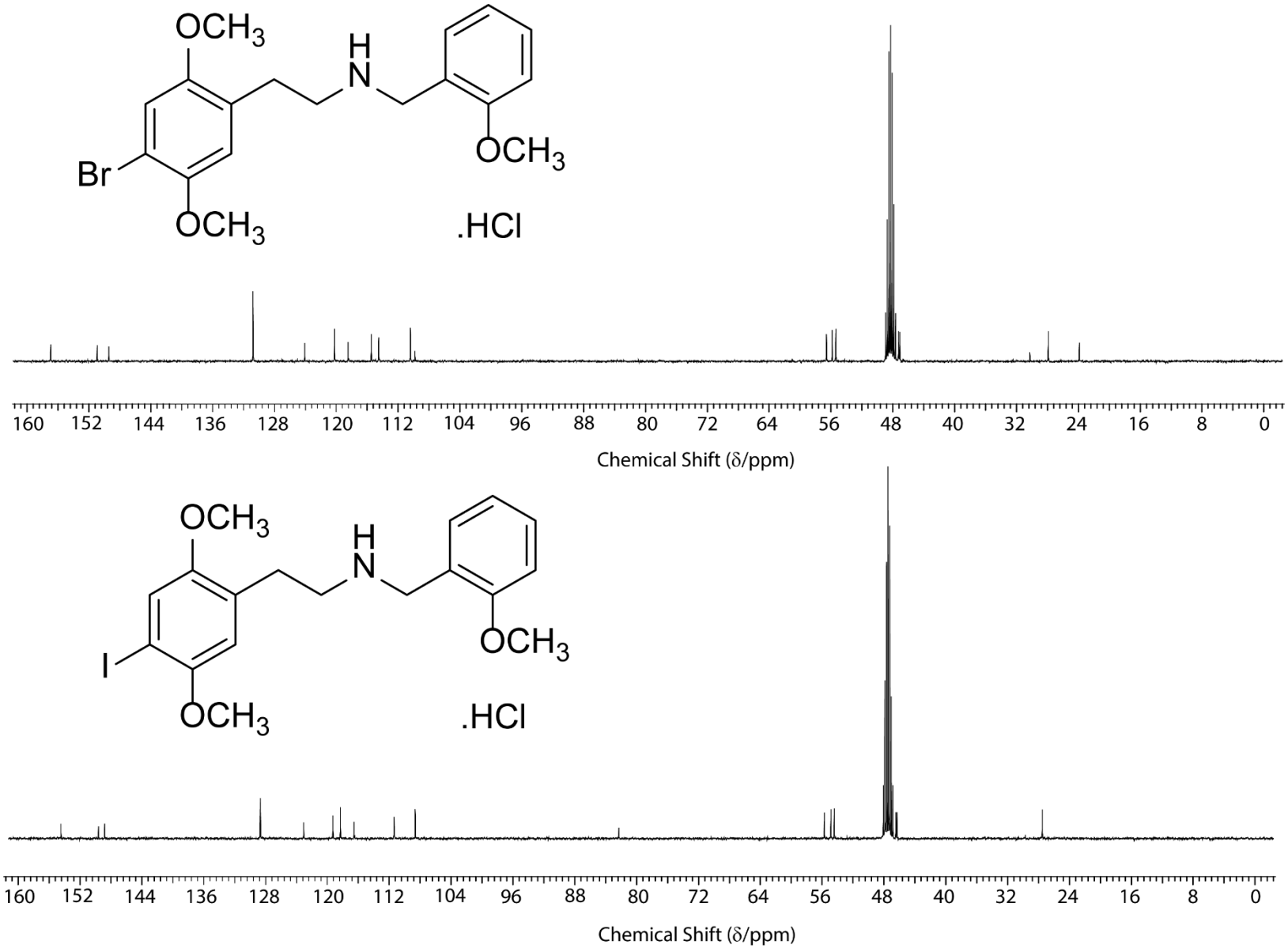

Figure S9. ATR-FT-IR spectrum of 2-(4-fluoro-2,5-dimethoxyphenyl)-N-(2-methoxybenzyl)ethan-1-amine.HCl (**2a**, 25F-NBOMe.HCl).

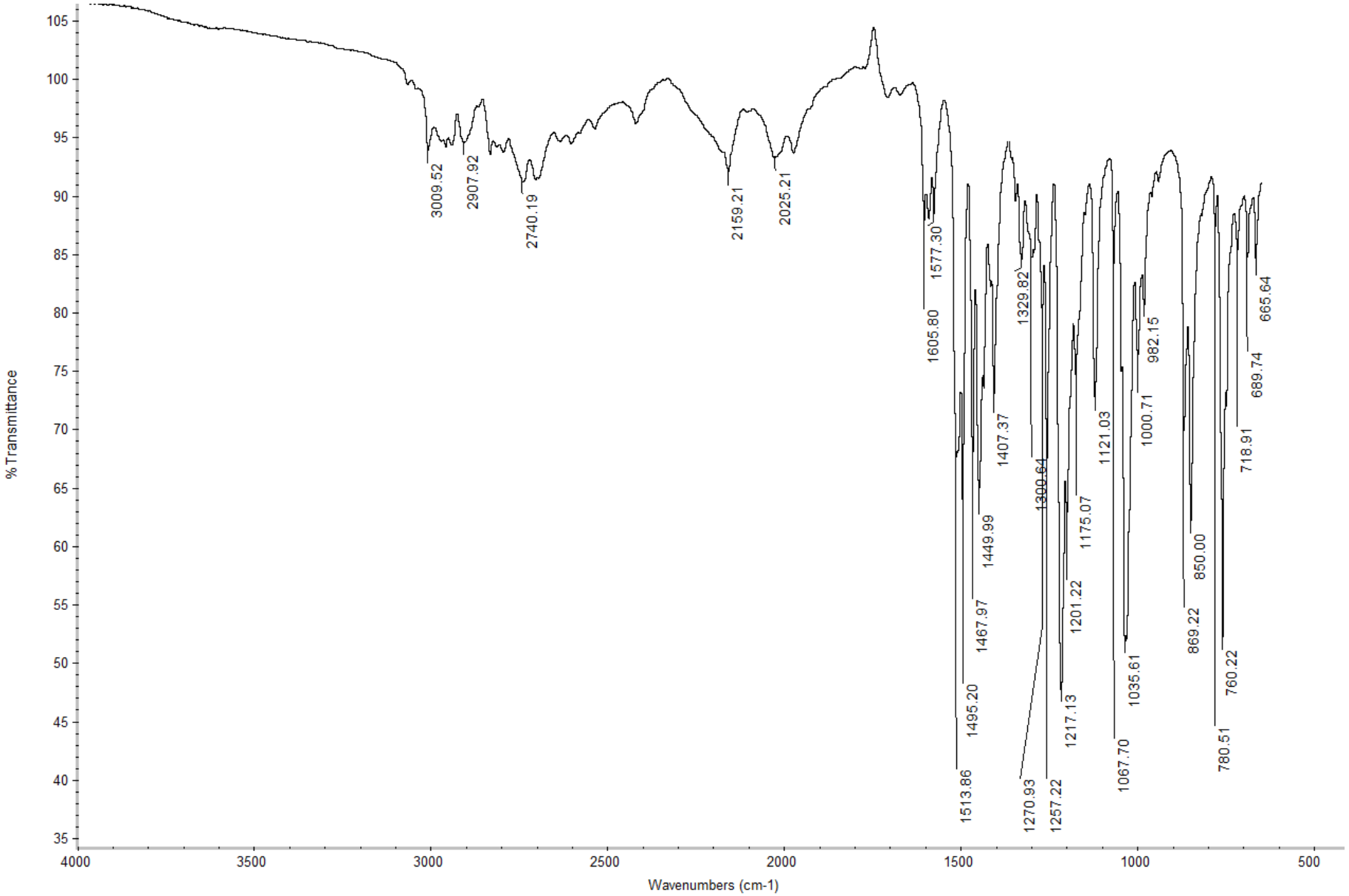

Figure S10. ATR-FT-IR spectrum of 2-(4-chloro-2,5-dimethoxyphenyl)-N-(2-methoxybenzyl)ethan-1-amine.HCl (**2b**, 25C-NBOMe.HCl).

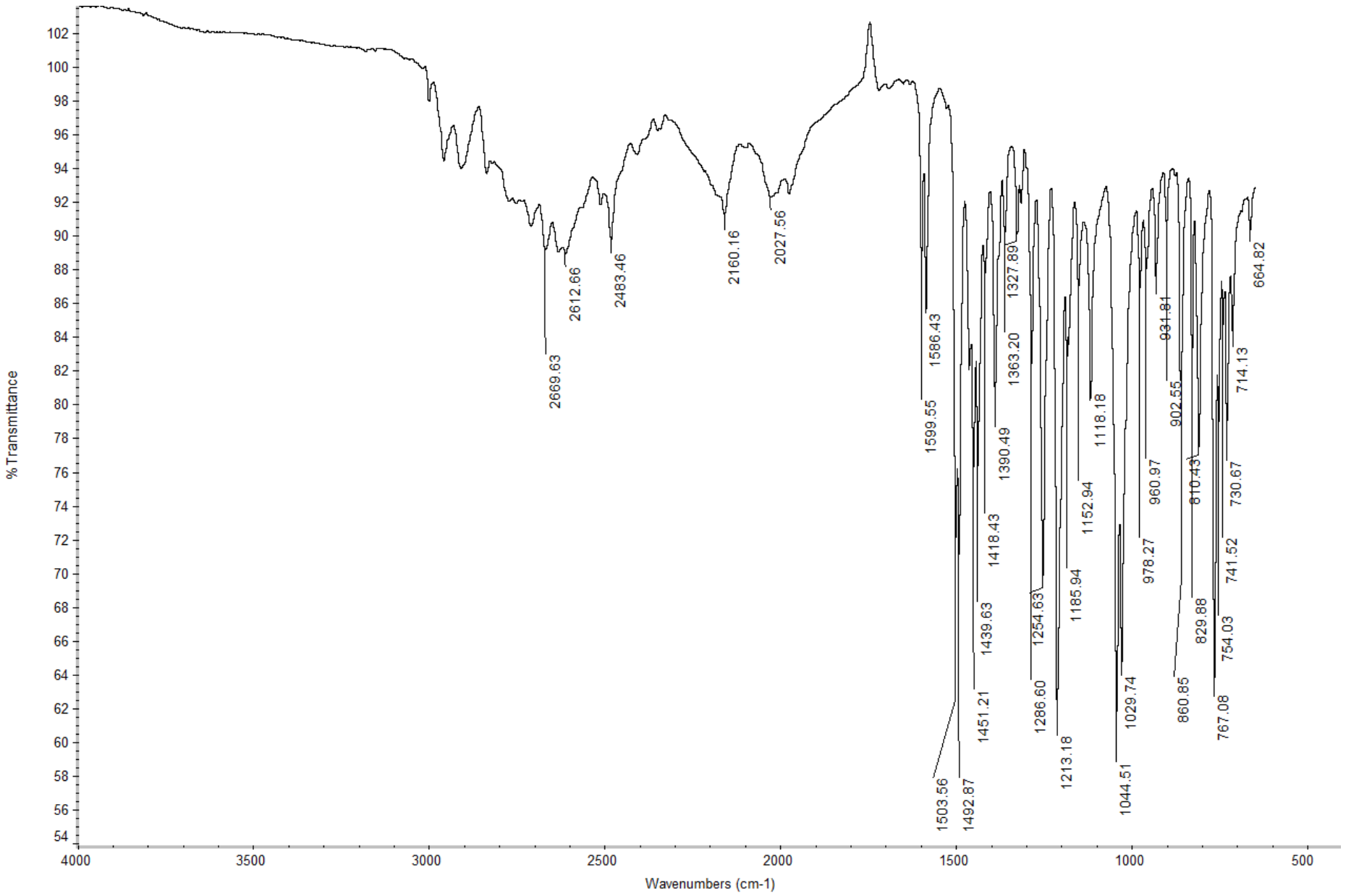

Figure S11. ATR-FT-IR spectrum of 2-(4-bromo-2,5-dimethoxyphenyl)-N-(2-methoxybenzyl)ethan-1-amine.HCl (**2c**, 25B-NBOMe.HCl).

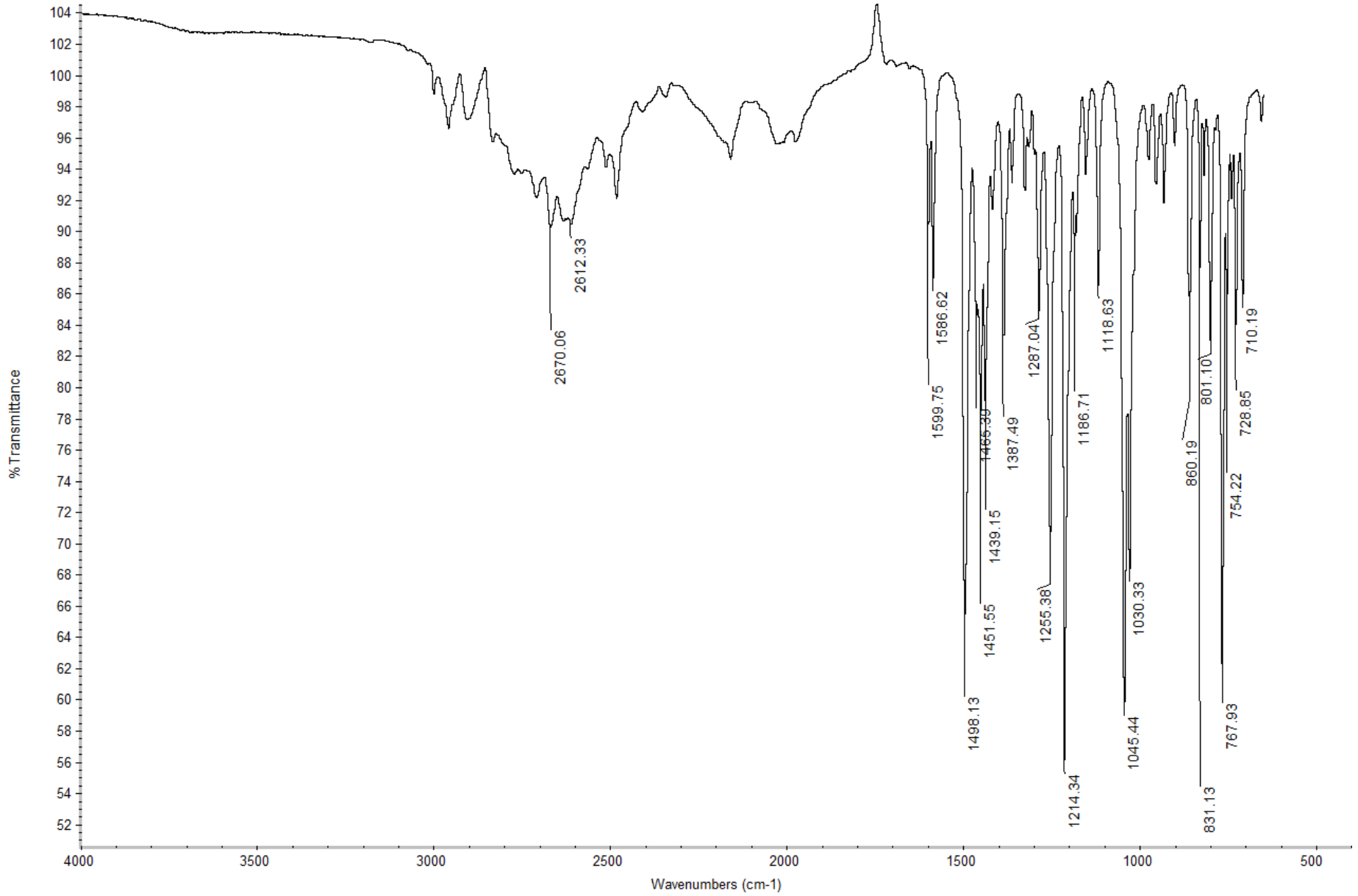

Figure S12. ATR-FT-IR spectrum of 2-(4-iodo-2,5-dimethoxyphenyl)-N-(2-methoxybenzyl)ethan-1-amine.HCl (**2d**, 25I-NBOMe.HCl).

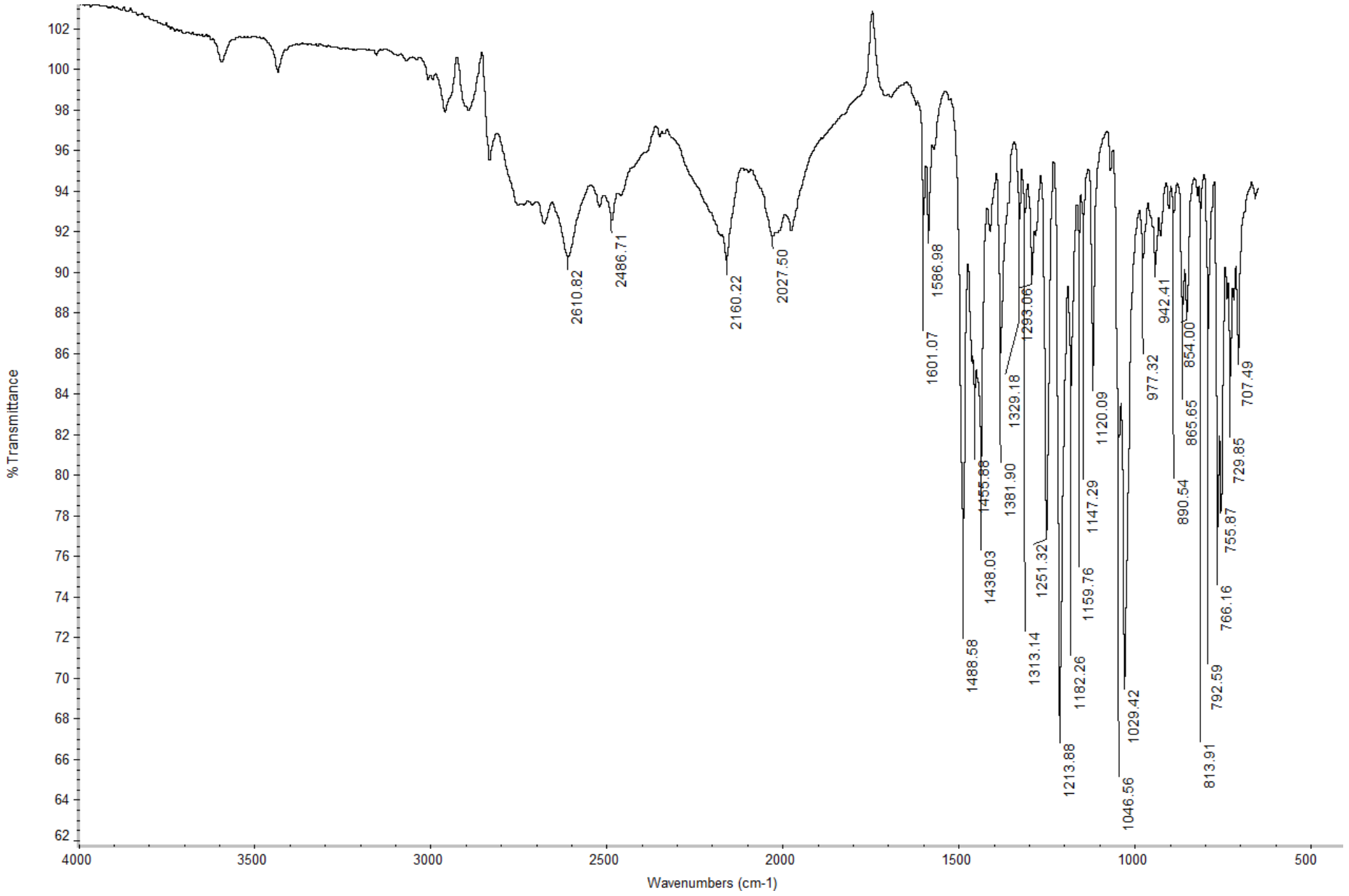

Figure S13. GC-EI-MS spectra of 2-(4-fluoro-2,5-dimethoxyphenyl)-N-(2-methoxybenzyl)ethan-1-amine.HCl (**2a**, 25F-NBOMe.HCl); 2-(4-chloro-2,5-dimethoxyphenyl)-N-(2-methoxybenzyl)ethan-1-amine.HCl (**2b**, 25C-NBOMe.HCl); 2-(4-bromo-2,5-dimethoxyphenyl)-N-(2-methoxybenzyl)ethan-1-amine.HCl (**2c**, 25B-NBOMe.HCl) and 2-(4-iodo-2,5-dimethoxyphenyl)-N-(2-methoxybenzyl)ethan-1-amine.HCl (**2d**, 25I-NBOMe.HCl).

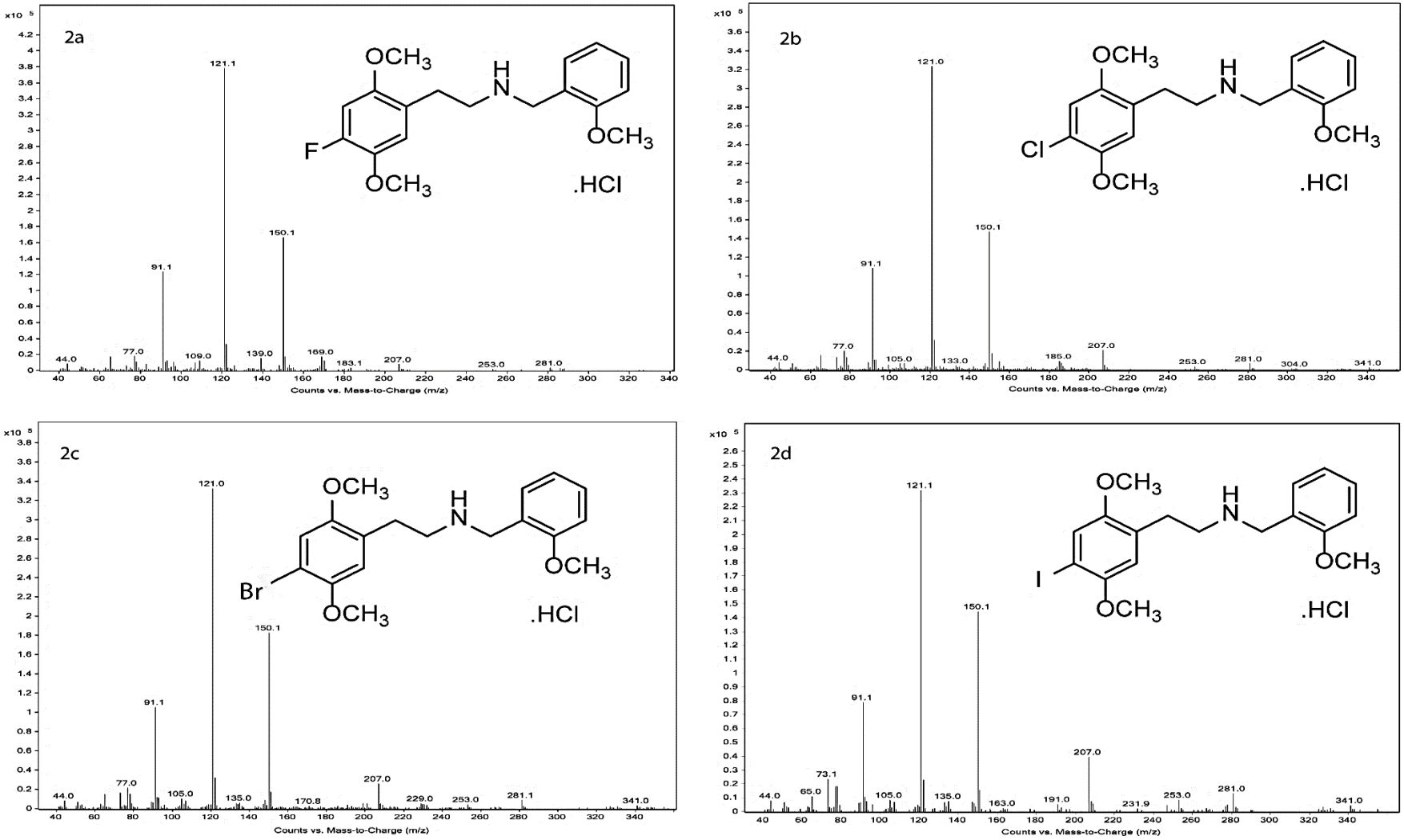

References

1. Mohamed, M.A.; Atty, S.A.; Yehia, A.M.; Foster, C.W.; Banks, C.E. and Allam, N.K. "Electrochemical Determination of the Serotonin Reuptake Inhibitor, Dapoxetine, Using Cesium–Gold Nanoparticles" ***ACS Omega***, 2 (10), 6628-6635, (2017).
2. Mohamed, M.A.; El-Gendy, D.M.; Ahmed, N.; Banks, C.E. and Allam, N.K. "3D spongy graphene-modified screen-printed sensors for the voltammetric determination of the narcotic drug codeine" ***Biosens Bioelectron***, 101 (Supplement C), 90-95, (2018).
3. Zuway, K.Y.; Smith, J.P.; Foster, C.W.; Kapur, N.; Banks, C.E. and Sutcliffe, O.B. "Detection and quantification of new psychoactive substances (NPSs) within the evolved "legal high" product, NRG-2, using high performance liquid chromatography-amperometric detection (HPLC-AD)" ***Analyst***, 140 (18), 6283-6294, (2015).
4. Smith, J.P.; Metters, J.P.; Irving, C.; Sutcliffe, O.B. and Banks, C.E. "Forensic electrochemistry: the electroanalytical sensing of synthetic cathinone-derivatives and their accompanying adulterants in "legal high" products" ***Analyst***, 139 (2), 389-400, (2014).
5. Câmpean, A.; Tertiş, M. and Săndulescu, R. "Electrochemical behavior of some purine derivatives on carbon based electrodes" ***Cent Eur J Chem***, 9 (3), 466-473, (2011).
6. Lourenção, B.C.; Medeiros, R.A.; Rocha-Filho, R.C.; Mazo, L.H. and Fatibello-Filho, O. "Simultaneous voltammetric determination of paracetamol and caffeine in pharmaceutical formulations using a boron-doped diamond electrode" ***Talanta***, 78 (3), 748-752, (2009).